22 Gb/s error-free data transmission beyond 1 km of multi-mode fiber using 850 nm VCSELs

Rashid Safaisini*, Krzysztof Szczerba, Erik Haglund, Petter Westbergh, Johan S. Gustavsson, Anders Larsson, and Peter A. Andrekson
Department of Microtechnology and Nanoscience, Photonics Laboratory, Chalmers University of Technology, Göteborg SE-412 96, Sweden

ABSTRACT

The first error-free data transmission beyond 1 km of multi-mode fiber at bit-rates exceeding 20 Gb/s is demonstrated using a high modulation bandwidth, quasi-single mode (SMSR~20 dB) 850 nm VCSEL. A VCSEL with small ~3 μm aperture shows quasi-single mode operation with a narrow spectral width. The top mirror reflectivity of the VCSEL is optimized for high speed and high output power by shallow etching. A combination of narrow spectral width and high optical power reduces the effects of fiber dispersion and fiber and connector losses and enables such a long transmission distance at high bit-rates.

Keywords: high-speed data communications, 850 nm VCSELs

1. INTRODUCTION

Optical interconnects are already taking over traditional speed-limited copper lines for petaflop and exaflop computational performance in today's supercomputers [1]. Fast development of cloud computing appeals high-speed optical links with up to 40 Gb/s single channel data transmission rate. This should allow short-reach rack-to-rack or module-to-module interconnects at such high speeds. However, longer reach optical links (up to ~2 km) at moderate bit-rates (20-25 Gb/s) come into the picture for applications in intra-building links in office areas and data centers where optical interconnects will be extended over a longer distance. Vertical-cavity surface-emitting lasers (VCSELs) operating at 850 nm have attracted much attention in data communications where reliability, efficiency, modulation speed, beam quality, and cost are of great importance. Owing to the well developed technology for 850 nm transceivers and more tolerant optical alignment of multi-mode fibers (MMFs), the combination of 850 nm VCSELs and MMFs has been the best solution for short-range high-speed optical interconnects for several years [2]. One of the major challenges in extending the reach of MMFs at high bit-rates arises from fiber bandwidth limitation caused by chromatic and modal dispersion. The effect of this limitation can be reduced by modifying MMF design and VCSEL modal properties. Compensation of chromatic dispersion by modal dispersion in graded-index MMFs was already shown to increase the effective modal bandwidth of the fiber to above 4700 MHz·km in OM4 MMF [3]. Moreover, reducing the number of transverse modes in the VCSEL, and consequently its emission spectral width, will reduce the effects of chromatic dispersion. It also reduces the effects of modal dispersion since a smaller number of VCSEL modes excite a reduced number of fiber modes. This leads to even higher effective modal bandwidth for the fiber. Integrating a mode filter with the VCSEL to suppress higher order modes [4] and employing small aperture VCSELs to support a smaller number of lasing modes [5-8] have already been shown to be successful for realizing single- or quasi-single mode VCSELs for high-speed extended-reach data communications. The latter offers a less complex approach for achieving the required modal properties even though there might be some reliability concerns with small aperture VCSELs [9]. This paper presents recent data on extending the reach of a MMF link to over 1 km at data transmission rates exceeding 20 Gb/s using a high-speed, small aperture 850 nm VCSEL. Figure 1 presents the state-of-the-art for transmission distance versus bit-rate for error-free (defined as bit-error rate (BER)<10^{-12}) operation when employing 850 nm VCSELs and more than 50 m length of MMF at room temperature.

*rashid.safaisini@chalmers.se; phone +46(0)31-772 1594

Vertical-Cavity Surface-Emitting Lasers XVII, edited by Kent D. Choquette, James K. Guenter,
Proc. of SPIE Vol. 8639, 86390T · © 2013 SPIE · CCC code: 0277-786X/13/$18
doi: 10.1117/12.2003693

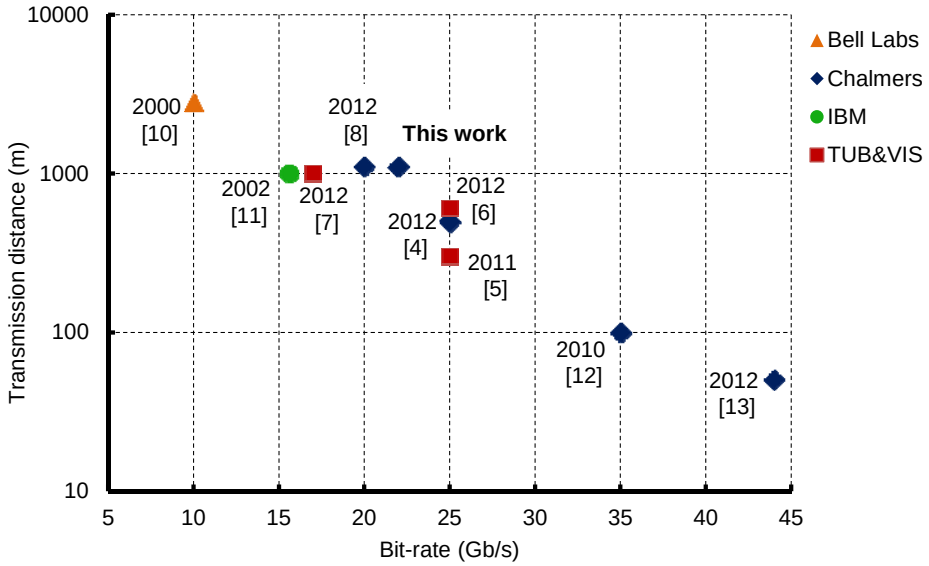

Figure 1. State-of-the-art for transmission distance vs. bit-rate for 850 nm VCSELs over >50 m MMF.

2. VCSEL DESIGN AND FABRICATION

2.1. Structure

The epitaxial structure consists of an n-type bottom distributed Bragg reflector (DBR) with Si-doped AlAs/$Al_{0.12}Ga_{0.88}As$ as the majority part to allow for a high thermal conductivity mirror for more efficient heat transport through the VCSEL bottom part. The active region employs five strained $In_{0.10}Ga_{0.90}As$ quantum wells separated by $Al_{0.37}Ga_{0.63}As$ barriers in a graded separate confinement heterostructure region. The p-type upper DBR contains C-doped $Al_{0.90}Ga_{0.10}As/Al_{0.12}Ga_{0.88}As$ while two 98% AlGaAs layers adjacent to the active region allow for wet oxidation to form an aperture for current and optical confinement. Four additional 96% AlGaAs layers were also placed above the first two oxide layers to reduce the parasitic oxide capacitance. The p-DBR was terminated with a highly doped GaAs contact layer.

2.2. Fabrication

VCSELs were fabricated through a sequence of standard high-speed VCSEL process steps summarized below. As the first step, top metal ring contacts were formed by sputter deposition of Ti/Au on the cap layer. VCSEL mesas were then defined by dry etching of the patterned surface in an inductively coupled plasma (ICP) system using $SiCl_4$/Ar and Cl_2/Ar gas mixtures. The etch depth was precisely determined by in-situ monitoring of the surface reflection using a laser and a photodetector. Next, the oxide apertures were formed by selective wet oxidation at 420 °C. The oxidation process was monitored using an IR microscope to form 2-4 μm aperture VCSELs in 22 μm diameter mesas for (quasi) single-mode operation and yet decent output power. In the next step, a deeper mesa with 50 μm diameter was dry-etched down to a 1-μm thick n-GaAs contact layer using the ICP system and the same gas mixture as used for the shallow mesa etch. The n-type contact was formed by electron-beam evaporation of Ni/Ge/Au on the patterned contact layer followed by metal lift-off and contact annealing at 420 °C in an N_2 environment. After removing the contact layer under the signal pad, the VCSELs were planarized with benzocyclobutene (BCB) and a Ti/Au bondpad was sputter deposited on the BCB to form a GSG contact configuration. A cross-section and top microscope view of a complete VCSEL is depicted in Figure 2.

To provide a higher output power for fiber transmission, and improved slope efficiency and modulation bandwidth, the top mirror reflectivity and thus cavity photon lifetime was adjusted by shallow etching of the top mesa surface [14]. Having a high launched power is important to overcome the fiber and connector losses for long fiber transmission.

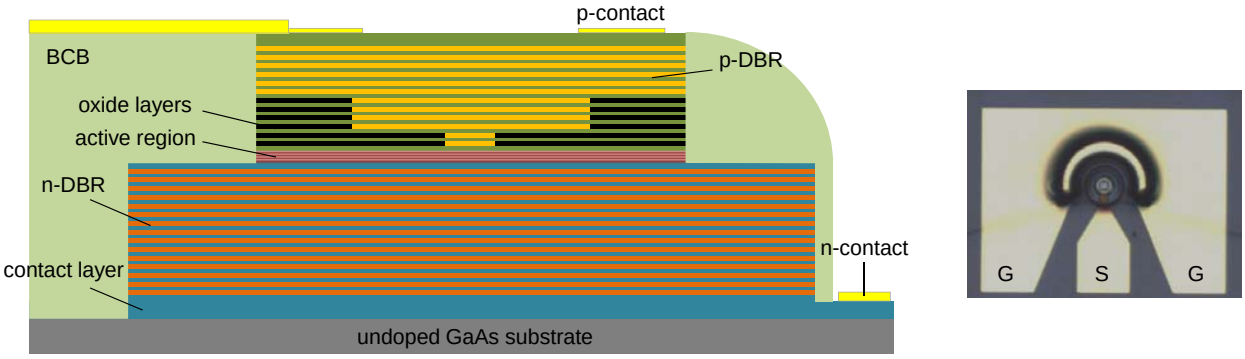

Figure 2. A cross-section (left) and top microscope view (right) of a fabricated VCSEL.

3. VCSEL CHARACTERIZATION

3.1. DC Characterization

The light-current-voltage (LIV) characteristics of a ~3 µm oxide aperture diameter VCSEL at 20 °C and the optical spectra at 1 and 3 mA are presented in Figure 3. The VCSEL shows a slope efficiency of 0.64 W/A with 0.19 mA threshold current and ~230 Ω differential resistance. The output power measured by a calibrated wide area silicon photodetector reaches the thermal roll-over value of 2 mW at 5.7 mA. The VCSEL operates primarily in the fundamental mode with a side-mode suppression ratio (SMSR) of 33 and 18 dB at 1 and 3 mA, respectively. The corresponding RMS spectral width ($\Delta\lambda_{rms}$) is 0.18 and 0.3 nm. The reduced VCSEL spectral width directly reduces the effects of chromatic fiber dispersion while it also reduces the effects of modal dispersion since the quasi-single mode VCSEL excites a reduced number of fiber modes. This leads to a higher effective modal bandwidth for the fiber and longer transmission distance.

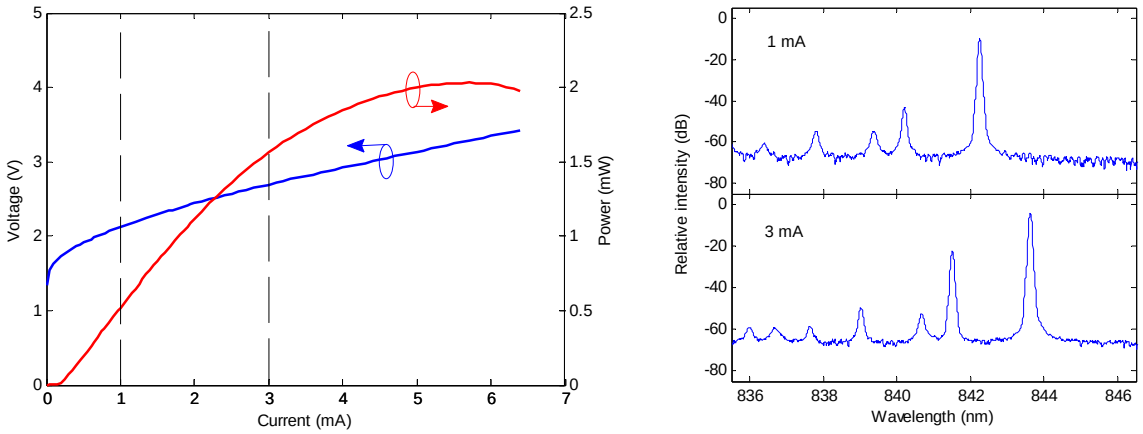

Figure 3. LIV curves (left) and optical spectra (right) of a ~3 µm oxide aperture VCSEL after top DBR reflectivity adjustment.

3.2. AC Characterization

VCSELs presented here are based on the same epitaxial material as the previously reported 7 µm nominal oxide aperture VCSEL with a 23 GHz 3 dB frequency response (f_{3dB}) and optimized photon lifetime [14]. The modulation bandwidth of the ~3 µm aperture VCSEL was measured using a 65 GHz Anritsu 3797C vector network analyzer and a 25 GHz bandwidth GaAs 1481 pin photodetector from New Focus with a responsivity of 0.4 A/W at 850 nm. The measured response is then corrected for the frequency responses of the photodetector and the high speed GSG probe.

A second order system transfer function derived from the single-mode rate equations, with an additional pole accounting for the effects of electrical parasitics and carrier transport with a cut-off frequency f_p (Equation 1), is then fitted to the modulation responses to extract the resonance frequency, f_r, and damping factor, γ, at each bias current. In Figure 4, f_{3dB} and f_r are plotted as a function of square root of current above threshold and reach their maximum values of 21 and 25 GHz, respectively. The modulation current efficiency factor (MCEF) and D-factor, respectively defined by f_{3dB}=MCEF·$(I-I_{th})^{½}$ and f_r=D·$(I-I_{th})^{½}$, were extracted from the low current part of the plots before saturation as MCEF=21.9 GHz/mA^{½} and D=17.3 GHz/mA^{½}. These two parameters are of importance for VCSEL dynamics and describe how fast f_{3dB} and f_r increase with increasing bias current, I, above the threshold current, I_{th}.

$$H(f) = \text{const} \times \frac{f_r^2}{f_r^2 - f^2 + j(f/2\pi)\gamma} \times \frac{1}{1 + j(f/f_p)} \tag{1}$$

Achieving high resonance frequencies at low bias currents, and therefore a large D-factor, is desired for high-speed modulation. It is also essential for high energy efficiency at high bit-rates since a high f_r, and therefore a high modulation bandwidth, can be reached at a lower bias current and voltage. The D-factor can be increased by improving internal quantum efficiency and differential gain, and by reducing the cavity volume [15] through proper epitaxial design and small aperture diameters. A large D-factor and high slope efficiency enable high modulation bandwidth and output power at low bias currents, which lead to low power consumption in high-speed data transmission.

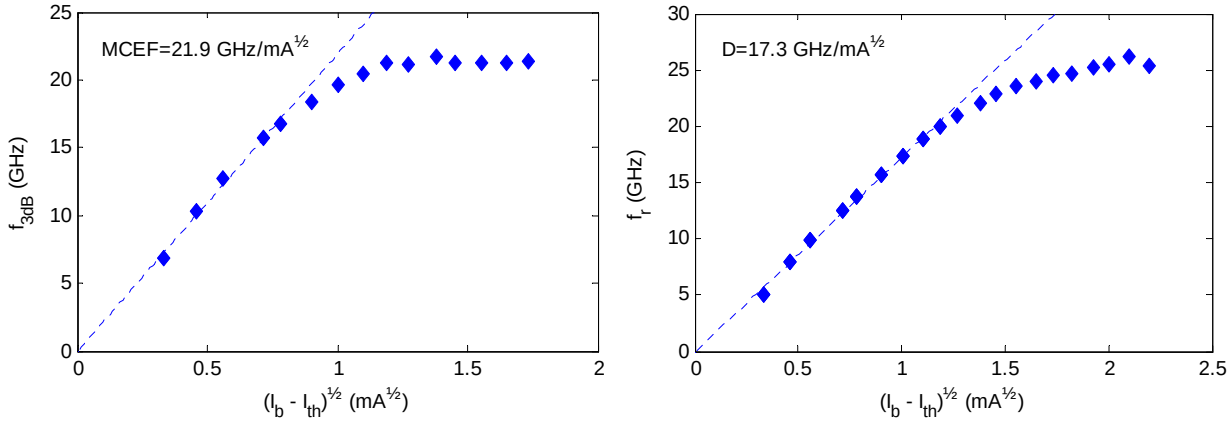

Figure 4. 3 dB (left) and resonance frequency (right) as a function of square root of bias current above threshold.

The damping factor can be written as a function of resonance frequency squared, γ=K·f_r^2+γ_0, where the K-factor describes the rate at which damping increases with resonance frequency and γ_0 is the damping factor offset which is important at low bias currents where f_r is small. A small K-factor, and thus small damping, is essential for realizing high modulation bandwidth VCSELs. However, a certain amount of damping is needed to prevent excessive ringing and timing jitter. Therefore, there is an optimum amount of damping for a given bit-rate. The present VCSEL has K=0.17 ns and γ_0=6.8 ns^{-1}.

3.3. Large Signal Analysis

The large signal modulation of the small aperture VCSEL was characterized at 20 °C by recording eye diagrams and measuring BERs for back-to-back (BTB) transmission and after up to 1100 m transmission over Draka MaxCap-OM4 MMF. The measurement set-up for this experiment is depicted in Figure 5.

A non-return-to-zero data pattern with a 2^7-1 bits long pseudorandom binary sequence, generated by an SHF 12103A bit pattern generator, was fed to the VCSEL through a linear SHF 807 amplifier with 24 dB gain in combination with a total of 23 dB attenuation and a 30 GHz SHF 120A bias-T via the GSG high speed probe. The linear amplifier was employed to suppress unwanted microwave reflections resulting from the VCSEL impedance mismatch to 50 Ω. The light output was butt-coupled to a 62.5 µm core diameter MMF which was aligned for maximum coupled power, before

launching to a 50 µm core diameter OM4 MMF. A combination of 300 and 800 m fiber spools was used for the 1100 m fiber transmission experiment. The fiber was then connected to a JDSU OLA-54 variable optical attenuator to vary the received optical power at the photoreceiver input for the BER measurement. The photoreceiver package used for the transmission experiments contains a New Focus 1580 photodiode with a nominal bandwidth of 12 GHz and a responsivity of 0.4 A/W at 850 nm, and an integrated transimpedance amplifier. The actual response of the photoreceiver showed a 3 dB bandwidth of 10 GHz and a 6 dB cut-off frequency of 14 GHz. The use of an integrated amplifier in the photoreceiver package can effectively reduce the noise level and improve the signal quality by better impedance matching for reduced microwave reflections. However, the photoreceiver available at the time of this experiment has a limited bandwidth which affects measurements at high bit-rates.

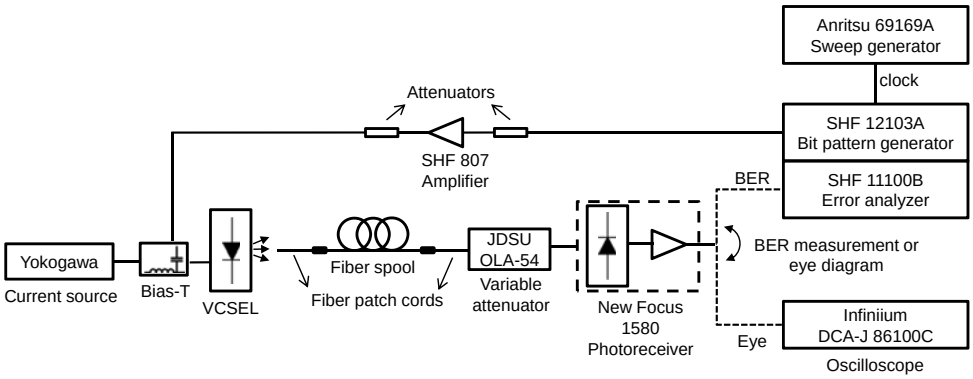

Figure 5. Set-up used for the large signal modulation measurements.

The output electrical signal of the photoreceiver was used to record eye diagrams using an Agilent Infiniium DCA-J 86100C 70 GHz digital communications analyzer or to perform BER analysis using an SHF 11100B error analyzer. The VCSEL was biased at 2.7 mA and the peak-to-peak modulation voltage measured at the high-speed probe was 0.95 V. The bias current and the modulation voltage were adjusted to give the best quality eyes. The VCSEL energy dissipation, defined as dissipated power/bit-rate, is 250 fJ/bit for data transmission at 22 Gb/s.

Inverted eyes and results from BER measurements for data rates of 20 and 22 Gb/s are shown in Figure 6 for BTB transmission and after transmission over 1100 m of OM4 MMF. Open eyes and error-free operation were achieved for transmission up to 1100 m at both data rates. However, the eyes at 22 Gb/s and long fiber suffer from intersymbol interference, which limits the transmission distance at data rates exceeding 22 Gb/s. A power penalty of approximately 2 dB is observed when increasing the transmission distance from BTB to 1100 m, at which the received optical power for BER=10^{-12} is below -7 dBm at 20 Gb/s and about -6 dBm at 22 Gb/s.

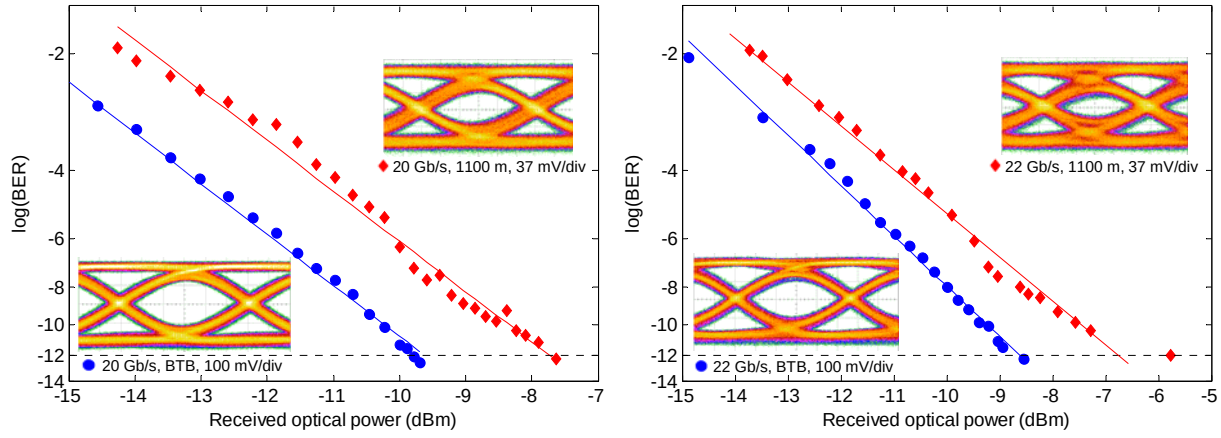

Figure 6. BER results and eye diagrams for BTB transmission and after 1100 m fiber transmission at 20 Gb/s (left) and 22 Gb/s (right).

4. CONCLUSIONS

High-speed, quasi-single mode 850 nm VCSELs were presented for increasing the reach of data communication links at high bit-rates. An output power of 2 mW was obtained for a ~3 μm oxide aperture VCSEL by adjusting the top mirror reflectivity to overcome power loss in the fiber and connectors. Simultaneously, the VCSEL operated with a limited number of modes with SMSR>18 dB and a narrow spectral width of $\Delta\lambda_{rms}$<0.29 nm at <3 mA bias current. The modulation bandwidth exceeded 20 GHz. This enabled error-free data transmission over >1 km OM4 MMF at >20 Gb/s. Data transmission at bit-rates exceeding 22 Gb/s over 1 km of MMF was mainly limited by the bandwidth of the photoreceiver used in the experiment. By employing a photoreceiver with higher bandwidth, one can expect to increase the bit-rate (to ~25 Gb/s) over 1 km of MMF using the VCSEL presented here. Utilizing quasi-single mode VCSELs with even higher output power and narrower spectral width can facilitate transmission over even longer MMFs at high bit-rates.

Acknowledgment

The authors would like to thank IQE Europe Ltd. for providing the epitaxial growth. This work was supported by the Swedish Foundation for Strategic Research (SSF).

REFERENCES

[1] C. Schow, F. Doany, and J. Kash, "Get On The Optical Bus," *IEEE Spectrum,* vol. 47, no. 9, pp. 32-56, Sep. 2010.

[2] M. A. Taubenblatt, "Optical Interconnects for High-Performance Computing," *Journal of Lightwave Technology*, vol. 30, no. 4, pp. 448–457, Feb. 2012.

[3] A. Gholami, D. Molin, and P. Sillard, "Compensation of Chromatic Dispersion by Modal Dispersion in MMF- and VCSEL-Based Gigabit Ethernet Transmissions," *IEEE Photonics Technology Letters*, vol. 21, no. 10, pp. 645–647, Jun. 2009.

[4] E. Haglund, Å. Haglund, P. Westbergh, J. S. Gustavsson, B. Kögel, and A. Larsson, "25 Gbit/s transmission over 500 m multimode fibre using 850 nm VCSEL with integrated mode filter," *Electronics Letters*, vol. 48, no. 9, pp. 517–518, Apr. 2012.

[5] G. Fiol, J. A. Lott, N. N. Ledentsov, and D. Bimberg, "Multimode optical fibre communication at 25 Gbit/s over 300 m with small spectral-width 850 nm VCSELs," *Electronics Letters*, vol. 47, no. 14, pp. 810–811, Jul. 2011.

[6] J. A. Lott, P. Moser, A. Payusov, S. Blokhin, P. Wolf, G. Larisch, N. N. Ledentsov, and D. Bimberg, "Energy efficient 850 nm VCSELs operating error-free at 25 Gb/s over multimode optical fiber up to 600 m," in *Proc. IEEE Optical Interconnects Conference*, pp. 42–43, 2012.

[7] P. Moser, P. Wolf, J. A. Lott, G. Larisch, A. Payusov, A. Mutig, W. Unrau, N. N. Ledentsov, W. Hofmann, and D. Bimberg, "High-speed VCSELs for energy efficient computer interconnects," *Proc. SPIE*, vol. 8432, pp. 843202-1–843202-8, 2012.

[8] R. Safaisini, K. Szczerba, E. Haglund, P. Westbergh, J. S. Gustavsson, A. Larsson, and P. A. Andrekson, "20 Gbit/s error-free operation of 850 nm oxide-confined VCSELs beyond 1 km of multimode fibre," *Electronics Letters*, vol. 48, no. 19, pp. 1225–1227, Sep. 2012.

[9] B. M. Hawkins, R. A. Hawthorne, J. K. Guenter, J. A. Tatum, and J. R. Biard, "Reliability of various size oxide aperture VCSELs," in *Proc. 52nd Electronic Components and Technology Conference,* pp. 540–550, 2002.

[10] G. Giaretta, R. Michalzik, and A. J. Ritger, "Long distance (2.8 km), short wavelength (0.85 μm) data transmission at 10 Gb/sec over new generation high bandwidth multimode fiber," *Conference on Lasers and Electro-Optics (CLEO)*, pp. 678–679, 2000.

[11] P. Pepeljugoski, D. Kuchta, Y. Kwark, P. Pleunis, and G. Kuyt, "15.6-Gb/s Transmission Over 1 km of Next Generation Multimode Fiber," *IEEE Photonics Technology Letters*, vol. 14, no. 5, pp. 717–719, May 2002.

[12] P. Westbergh, J. S. Gustavsson, B. Kögel, Å. Haglund, A. Larsson, A. Mutig, A. Nadtochiy, D. Bimberg, and A. Joel, "40 Gbit/s error-free operation of oxide-confined 850 nm VCSEL," *Electronics Letters*, vol. 46, no. 14, pp. 1014–1015, Jul. 2010.

[13] P. Westbergh, R. Safaisini, E. Haglund, J. S. Gustavsson, A. Larsson, M. Geen, R. Lawrence, and A. Joel, "High-Speed Oxide Confined 850-nm VCSELs Operating Error-Free at 40 Gbit/s up to 85°C," *IEEE Photonics Technology Letters,* submitted for publication, 2012.
[14] P. Westbergh, J. S. Gustavsson, B. Kögel, Å. Haglund, and A. Larsson, "Impact of Photon Lifetime on High-Speed VCSEL Performance," *IEEE Journal of Selected Topics in Quantum Electronics*, vol. 17, no. 6, pp. 1603–1613, Dec. 2011.
[15] L. Coldren and S. Corzine, *Diode Lasers and Photonic Integrated Circuits*. New York: Wiley, 1995.